Electronic structures of disordered Ag–Mg alloys

R. G. Jordan, Yan Liu,* and S. L. Qiu
Alloy Research Center, Department of Physics, Florida Atlantic University, Boca Raton, Florida 33431-0991

B. Ginatempo and E. Bruno
Dipartimento di Fisica, Università di Messina, Cassella Postale 50, I-98166 S. Agata, Messina, Italy

G. M. Stocks and W. A. Shelton
Oak Ridge National Laboratory, Oak Ridge, Tennessee 37831
(Received 3 June 1994)

We have calculated the electronic structures of the valence bands in a series of α-phase (disordered fcc) Ag-Mg alloys over the range 0–30 at. % Mg using the Korringa-Kohn-Rostoker method within the coherent potential approximation (KKR-CPA). We find that the variation of the equilibrium lattice constant with composition is in good agreement with experimental measurements. The bandwidth of the Ag-related d states decreases with the addition of Mg although the position of the bottom of the band remains roughly fixed in energy with respect to the Fermi level; an observation that is consistent with photoemission measurements. The electronic spectral densities are very sharply peaked at the Fermi energy with widths that are $< 1\%$ of the Brillouin zone dimension and so the Fermi surfaces of the alloys are well defined throughout the zone. The radius of the neck at the L point and the belly radii in the ΓX and ΓK direction increases approximately linearly with increasing Mg content. Taking into account some previous work on the origin of short range order in Ag-rich alloys, we conclude that the local-density approximation KKR-CPA method provides a realistic description of the electronic structure in α-phase Ag-Mg alloys.

I. INTRODUCTION

Ag-rich Ag-Mg alloys exhibit a number of interesting properties. The binary phase diagram itself is relatively simple;[1] there is a disordered solid solution α phase (fcc structure) that extends up to nearly 30 at. % Mg and an ordered β' phase (CsCl structure) above ~40 at. % Mg. Within the α phase region an ordered α' phase occurs above ~20 at. % Mg; the ordering temperatures are strongly composition dependent with a maximum of ~390 °C near 24 at. % Mg. The two ordered phases are particularly interesting. The α' phase is a one-dimensional, long period superlattice (LPS), made up of domains, based on cells with the $L1_2$ structure, separated by antiphase boundaries.[2] The actual LPS structure depends on composition and thermal history, but the simplest is the DO_{23} structure that occurs near 24 at. % Mg. The β' phase remains ordered to its melting point. It has an electron-atom (e/a) ratio of 3/2 and is a member of a special class of alloys referred to as Hume-Rothery phases (or electron compounds) whose structures are strongly correlated with the e/a ratio.[3] We have recently reported[4] an investigation of the electronic structures in both of the ordered phases using a combination of ultraviolet and x-ray photoelectron spectroscopies and first-principles band structure and photocurrent calculations. Consequently, we now focus our attention on the electronic structure of the α-phase (disordered) alloys.

Some 25 years ago Ohshima and Watanabe[5] found that considerable short range order was present in α-phase alloys containing 11–28 at. % Mg. Using the Korringa-Kohn-Rostoker method within the local density and coherent potential approximations (LDA-KKR-CPA), we calculated the Fermi surfaces in a number of disordered Ag-Mg alloys and we provided very strong evidence[6–8] that the short range order is driven by a Fermi surface nesting mechanism. We showed that there are flattened and parallel regions of Fermi surface in the ΓK direction at which nesting could occur, giving rise to concentration waves and groups of intensity maxima in the diffuse scattering. The positions of the peaks in the diffuse scattering depend sensitively on the magnitude of the Fermi surface nesting vector and we found that our calculated values of the peak separations were in excellent agreement with the experimental measurements of Ohshima and Watanabe.[5] It *could* be argued therefore that such agreement provides an "indirect" confirmation that at least certain features of the calculated Fermi surfaces are correct. In this paper, we report the results of a more detailed investigation of the electronic structures in a number of disordered Ag-rich Ag-Mg alloys. We have used the LDA-KKR-CPA method to calculate the electronic spectral density throughout the Brillouin zone and we have made contact with experimental results wherever possible.

II. ELECTRONIC STRUCTURE CALCULATIONS

We calculated the valence band electronic structure in a series of (disordered fcc) Ag-Mg alloys in the range 10–

30 at.% Mg using the LDA-KKR-CPA method within the muffin-tin approximation.[9] (We also carried out similar calculations for Ag for comparative purposes.) The core states were treated fully relativistically and the valence band states were treated within the scalar relativistic approximation. At each composition we minimized the total energy as a function of lattice constant and obtained the corresponding self-consistent charge densities. We used the self-consistent output potential functions, etc., to calculate the densities of states and the electronic spectral densities along various symmetry directions in the (fcc) Brillouin zone. As we will describe in more detail later, we found that over the composition range we studied the widths of spectral density at the Fermi energy were very narrow — thus, the Fermi surfaces are well defined — and so we calculated the Fermi surfaces and determined various surface dimensions.

The most relevant physical quantity we deal with in this paper is the Bloch spectral function (BSF), $\mathcal{A}^B(\mathbf{k},\epsilon)$, which represents the density of electron states at energy ϵ and wave vector $\mathbf{k}$. In an ordered system the BSF can be expressed as a sum of δ functions:

$$\mathcal{A}^B(\mathbf{k},\epsilon)=\sum_\nu \delta(\epsilon-\epsilon_\nu(\mathbf{k})), \tag{1}$$

where $\epsilon_\nu(\mathbf{k})$ are the energy eigenvalues of the νth band, and the locus of the peaks in $(\epsilon,\mathbf{k})$-space trace the conventional band structure. Equivalently, for ordered systems we may write

$$\mathcal{A}^B(\mathbf{k},\epsilon)=-\frac{1}{\pi}\mathrm{Im}\left\{\lim_{\eta\to 0}\sum_\nu \frac{1}{\epsilon-\epsilon_\nu(\mathbf{k})+i\eta}\right\}. \tag{2}$$

In an alloy, $\mathrm{A}_{c_\alpha}\mathrm{B}_{c_\beta}$, the disorder broadens the peaks of $\mathcal{A}^B(\mathbf{k},\epsilon)$ and, as it has been shown,[9] in the coherent approximation the BSF is related to the coherent Green function:

$$\mathcal{A}^B(\mathbf{k},\epsilon)=-\frac{1}{\pi}\mathrm{Im}\{\mathrm{Tr}[\underline{G}^c(\mathbf{k},\mathbf{k}',\epsilon)]\}.$$

The total density of states, $n(\epsilon)$, can be expressed in terms of the averaged densities of states $\overline{n}_\alpha(\epsilon)$ and $\overline{n}_\beta(\epsilon)$, or directly from the BSF as an integral over the Brillouin zone:

$$n(\epsilon)=c_\alpha\overline{n}_\alpha(\epsilon)+c_\beta\overline{n}_\beta(\epsilon)=\frac{1}{\Omega_{\mathrm{BZ}}}\int \mathcal{A}^B(\mathbf{k},\epsilon)d\mathbf{k}. \tag{3}$$

In systems in which the disorder broadening is not too large, as in Ag-Mg alloys, the δ-function peaks in Eq. (1) are simply broadened and shifted in ϵ and $\mathbf{k}$ while remaining clearly identifiable with a Lorentzian shape. In this case, the Fermi surface of the alloy can be defined as the locus of the $\mathbf{k}$ peaks in the BSF at the Fermi energy, i.e., in $\mathcal{A}^B(\mathbf{k},\epsilon_F)$. Of course, in an alloy the eigenvalues $\epsilon_\nu(\mathbf{k})$ are no longer real and their imaginary part is proportional to the inverse of the quasiparticle lifetime,

$$\mathrm{Im}\{\epsilon_\nu(\mathbf{k})\}=\frac{\hbar}{\tau_\nu(\mathbf{k})}.$$

It is, therefore, more convenient to generalize Eq. (2) as

$$\mathcal{A}^B(\mathbf{k},\epsilon)=-\frac{1}{\pi}\mathrm{Im}\left\{\sum_\nu \frac{1}{\epsilon-\epsilon_\nu(\mathbf{k})}\right\}. \tag{4}$$

At a given $\mathbf{k}$ Eq. (4) gives a clear account of the Lorentzian structure of the peaks in the Bloch spectral function. Alternatively, the above picture may be "reversed" and, at a fixed energy, different, complex $\mathbf{k}$ points, coming from the continuation of the band structure, $\epsilon_\nu(\mathbf{k})$, give contributions to the BSF. The latter turns out to be "astigmatic," made up of Lorentzians centered about $\mathrm{Re}\{\mathbf{k}\}$ and with half widths related to $\mathrm{Im}\{\mathbf{k}\}$ and proportional to the inverse of the electron coherence length,

$$l_{coh}=\frac{\hbar}{\delta k}.$$

Therefore, the BSF may be decomposed as a sum of Lorentzian contributions:

$$\mathcal{A}^B(\mathbf{k},\epsilon)=\sum_{\nu=1}^{\nu_{\max}}\frac{C_\nu(\mathbf{k})}{[\epsilon-\mathrm{Re}\{\epsilon_\nu(\mathbf{k})\}]^2+[\mathrm{Im}\{\epsilon_\nu(\mathbf{k})\}]^2} \tag{5}$$

where the $C_\nu(\mathbf{k})$ weight each Lorentzian contribution to the BSF. In the case where on varying the energy at a given $\mathbf{k}$ one crosses a nearly vertical band, the tails of the Lorentzians corresponding to many other states close to $\epsilon_\nu(\mathbf{k})$ overlap. Thus, broad peaks will be produced that may lead to an overestimate of the width if we use Eq. (5) as a fit formula. On the other hand, in the case of (near) horizontal bands, the estimates of the widths from Eq. (5) are much more precise.

III. RESULTS AND DISCUSSION

In Fig. 1 we show the variation of the calculated equilibrium lattice constants with composition and compare the results with the experimental measurements of Fujiwara *et al.*[10] and Buckley *et al.*[11] The two variations are closely parallel — the slopes of the experimental

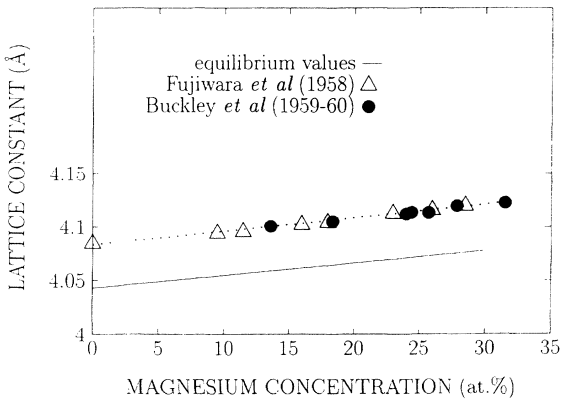

FIG. 1. A comparison of the calculated and experimentally determined lattice constants. The experimental results are from Refs. 10 and 11.

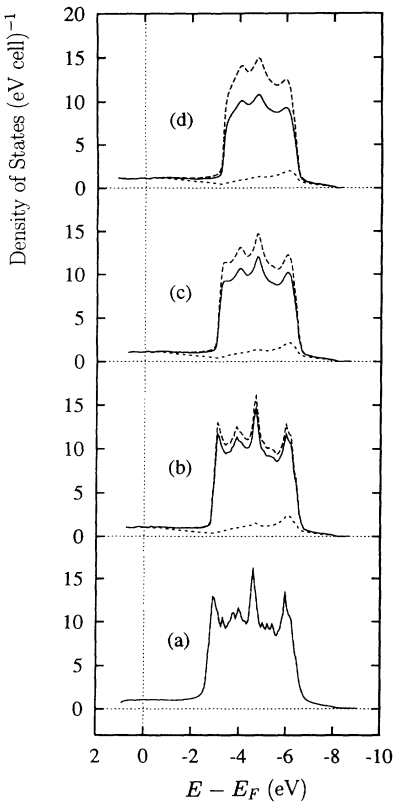

FIG. 2. The total and site decomposed densities of states, from Eq. (3) of (a) Ag, (b) Ag–10 at.% Mg, (c) Ag–20 at.% Mg, and (d) Ag–30 at.% Mg. The solid line is the total density of states $n(\epsilon)$, the heavier dashed line for the alloys is the density of states at the Ag site $\overline{n}_{Ag}(\epsilon)$, the lighter dashed line is that at the Mg-site $\overline{n}_{Mg}(\epsilon)$.

and calculated lines are 1.25×10^{-3} Å (at.%)$^{-1}$ and 1.17×10^{-3} Å (at.%)$^{-1}$, respectively — although the calculated values are ~1% lower than the measured values. One has to bear in mind, of course, that the calculations represent values at 0 K whereas the experimental values were obtained at room temperature. In addition, such discrepancies are typical for transition metals and alloys using a calculational scheme involving the local density and muffin-tin approximations. Thus, the agreement between the experimental and calculated results is in line with similar comparisons and can be therefore considered satisfactory although the local-density and muffin-tin approximations seem to overemphasize the bonding.

In Fig. 2 we show the site decomposed and total densities of states calculated using Eq. (3) ($\alpha \equiv$ Ag and $\beta \equiv$ Mg) for (a) pure Ag and for alloys containing, (b) 10 at.% Mg, (c) 20 at.% Mg, and (d) 30 at.% Mg. There are three points to be made about these plots:

(i) The major contribution to the density of states in the alloys comes from the Ag 4d-related states.

(ii) Although the bandwidth decreases from (a) to (d) — as the overlap of the Ag 4*d*-wave functions is reduced by dilution and the increase in lattice constant — the position of the bottom of the band, i.e., at the largest binding energy, remains roughly fixed in energy; in Table I we have listed the values of the bandwidth (i.e., the full width at half maximum) and the energy position of the bottom of the band.

(iii) An increase in the disorder broadening with increasing Mg concentration can be clearly seen.

Behavior similar to (i) and (ii) is observed in *uv* photoemission measurements[12] and we show in Fig. 3(a) comparison of ultraviolet photoemission spectra taken using He II radiation (40.8 eV) from pure Ag with that from a disordered alloy containing 25 at.% Mg and the corresponding densities of states. In order to make a proper comparison, both photoemission spectra were measured at a temperature of 420 °C, i.e., well above the disordering temperature of the alloy. Because of the energy-dependent effects of the electron-photon matrix elements and the finite hole lifetimes, and the finite resolution of the spectrometer, we cannot expect a direct, one-to-one correspondence between the shapes of the densities of states in Fig. 3(a) and the photoemission spectra in Fig. 3(b). Nevertheless, there is a reasonable level of agreement; in particular, the narrowing of the valence band and the "locking" of the position of the bottom of the band are clearly apparent in the data. (There is also a shift in energy between features in the experimental spectra and the densities of states; energy shifts are common in such comparisons and are probably due to self-energy effects.)

In Figs. 4 and 5 we show the Bloch spectral functions for the alloy containing 25 at.% Mg along the ΓX, ΓK, ΓL, and ΓLW directions in the fcc Brillouin zone. (The spectra functions are similar for all the alloys and we select the result for the 25 at.% Mg alloy as being typical.) In Fig. 4, we have also indicated by arrows the positions

TABLE I. Calculated values of the bandwidths and the positions of the bottom of the band, with reference to the Fermi energy, in disordered Ag-rich Ag-Mg alloys.

Composition (at.% Mg)	Bandwidth (eV)	Bottom of band (eV)
0.0	3.44	-6.25
10.0	3.37	-6.32
15.0	3.31	-6.34
20.0	3.24	-6.37
22.5	3.18	-6.39
25.0	3.13	-6.36
27.5	3.10	-6.34
30.0	3.00	-6.32

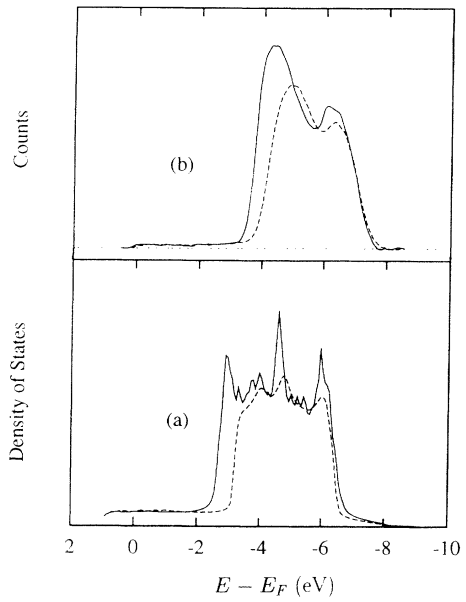

FIG. 3. A comparison of (a) the total densities of states and (b) photoemission spectra for Ag and Ag–25 at. % Mg. The photoemission spectra were obtained using He II radiation, Ref. 12.

of the eigenvalues for pure Ag. There are several points to note.

(i) It is apparent that the states of (essentially pure) s and p character show much less disorder broadening compared with those with d character. This is a real effect since the procedure used, based on scanning in ϵ at fixed $\mathbf{k}$, see Eq. (5), will actually tend to provide an overestimate of the broadening of the s/p states because their dispersion is much more rapid than that of the d states.

(ii) The reduction of the valence bandwidth on alloying is clearly evident in these plots. In addition, the shifts of the peak positions from the pure Ag eigenvalues increase with increasing energy from ~ 0 in the vicinity of Γ_1 but increasing to ~ 0.5 eV near E_F.

(iii) The states at the Fermi energy are of predominantly s/p character and are very sharp. Consequently the Fermi surface is well defined.

We have plotted the spectral function along ΓLW using a different perspective in Fig. 5, and it shows the presence of a neck on the Fermi surface at the L point.

We calculated also the spectral function at the Fermi energy, $\mathcal{A}^B(\mathbf{k}, \epsilon_F)$, in various planes in the Brillouin zone. Again, the results are similar for all the alloys and in Figs. 6(a), 6(b), and 6(c) we show the variation of $\mathcal{A}^B(\mathbf{k}, \epsilon_F)$ along radial directions in the ΓXKX, $\Gamma XULK$, and $LWKWU$ planes, respectively, for the 25 at. % Mg alloy. The widths, δk, of the peaks in the spectral function vary with $\mathbf{k}$, as shown in Fig. 7 for the ΓXKX plane, but they are considerably less than 1% of the Brillouin zone dimension for all the alloys studied. As a result the Fermi surfaces are well defined and they can be conveniently represented in $\mathbf{k}$ space by the locus of the maxima in $\mathcal{A}^B(\mathbf{k}, \epsilon_F)$. We show two sections so determined in Figs. 8(a) and 8(b); in Fig. 8(a) we compare the section in the ΓXKX plane with that obtained within the empty lattice approximation for the appropriate e/a ratio and we can see that it is "flattened" in the ΓK direction. The Fermi surfaces of the alloys resemble that in pure Ag with a neck at the L point; the major effect of adding Mg is to increase the enclosed volume. The neck is circular in section and in Figs. 9(a) and 9(b) we show how the neck radius and the belly radii in the ΓX and ΓK directions vary with composition. The variation in each case is very closely linear. We have also included values of the neck radii for Ag and Ag_3Mg (assuming

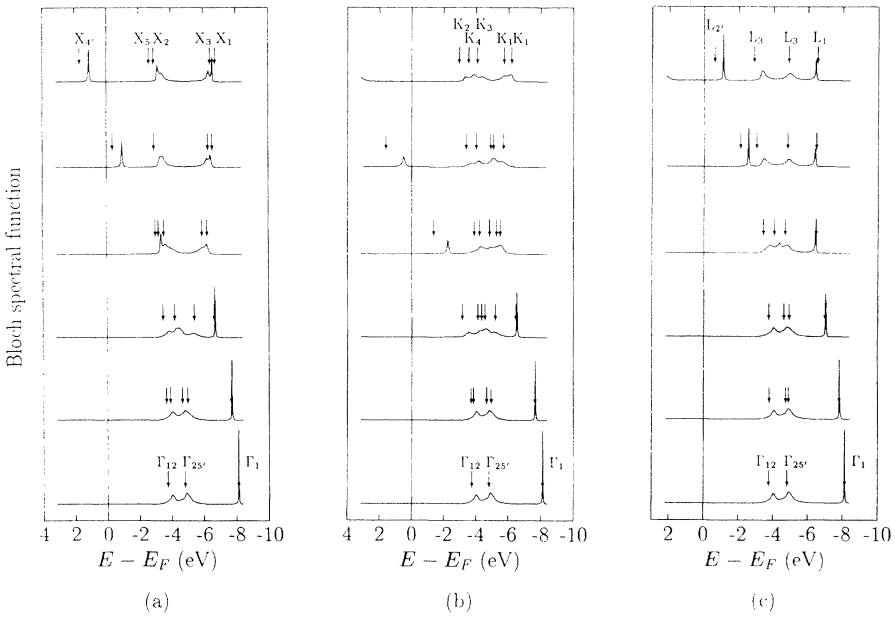

FIG. 4. The Bloch spectral function for Ag–25 at. % Mg for different $\mathbf{k}$ values along the (a) ΓX, (b) ΓK, and (c) ΓL directions. The lowest spectra are for the Γ point; the upper spectra are for (a) the X point, (b) the K point, and (c) the L point. The different $\mathbf{k}$ values in each case are equally spaced between the extremes. The arrows show the positions of the eigenvalues for pure Ag.

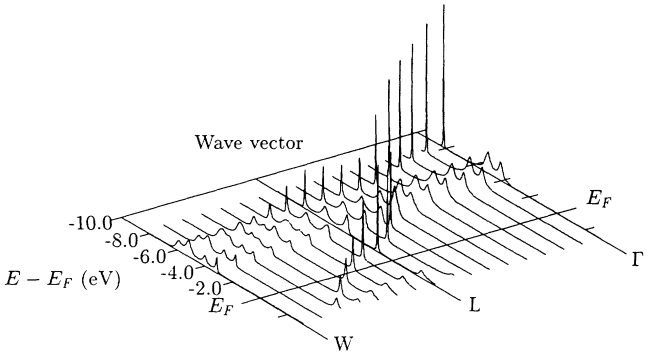

FIG. 5. The Bloch spectral function along ΓLW for Ag–25 at. % Mg.

the $L1_2$ structure) obtained using the linear muffin-tin orbital (LMTO) method.[4]

We expect that a Shockley-type surface state will occur on the (111) surfaces of the alloys, located in the "$L_2' - L_1$" s-p hybridization gap that spans the Fermi level.[13] The dispersion of this surface state in $(\epsilon, \mathbf{k}_{||})$ space will be governed by that of the uppermost occupied band along LW, shown in Fig. 5. Angle-resolved uv photoemission measurements on the (111) surface around normal emission would be a suitable probe of this behavior and might, therefore, permit an experimental investigation of the variation of the neck radii with composition.[14] (Conventional fermiology techniques, apart from 2D-angular-correlation-of-annihilation-radiation studies, are not generally suitable for such investigations because of the short lifetimes of states on the Fermi surface.) According to our calculations the neck radius in ordered Ag_3Mg ($L1_2$ structure) is very similar to that in the disordered alloy. The same result was inferred experimentally in the case of Cu_3Au; a study of the dispersion of the Shockley-type surface state on the (111) surface about the $\overline{\Gamma}$ point using angle-resolved uv photoelectron spectroscopy showed that the occupied "$\mathbf{k}_{||}$-extent" of the surface state was essentially the same in the ordered ($L1_2$ structure) and disordered (fcc) phases.[15]

As a result of recent investigations, we believe that the shape and size of the Fermi surfaces of α-phase Ag-Mg

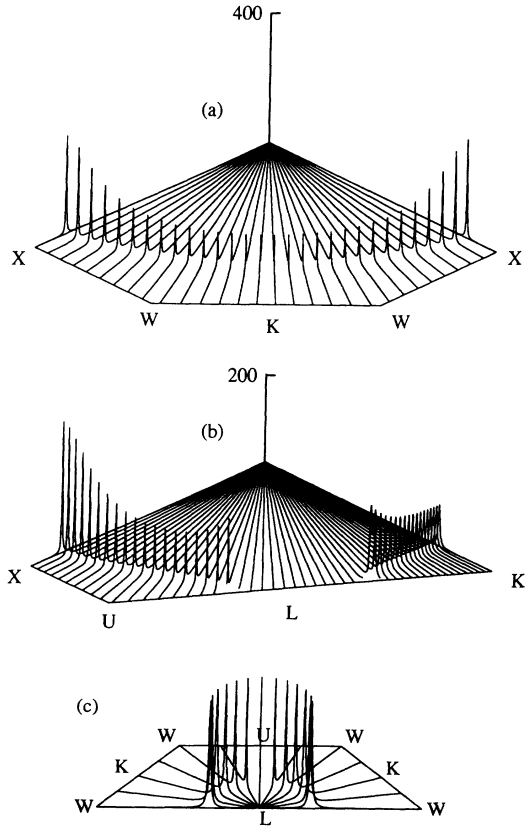

FIG. 6. The Bloch spectral function for Ag–25 at. % Mg at the Fermi energy in (a) the ΓXKX, (b) $\Gamma XULK$, and (c) $LWKWU$ planes.

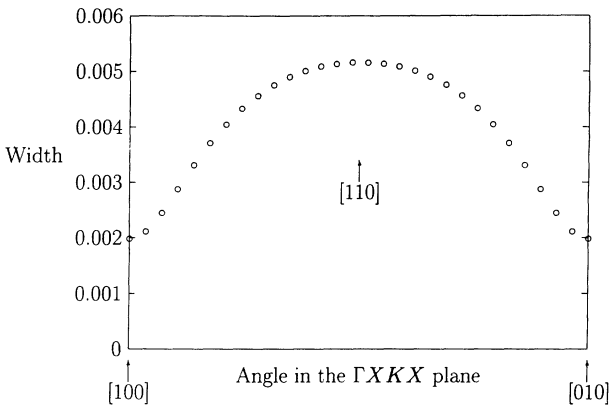

FIG. 7. The angular variation of the width of the Bloch spectral function for Ag–25 at. % Mg at the Fermi energy in the $\Gamma XWKX$ plane. The width is normalized to $|\Gamma X|$.

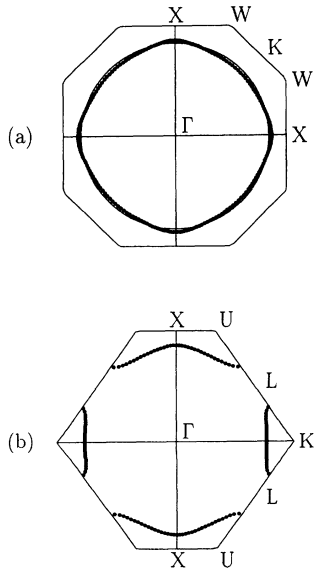

FIG. 8. Sections of the "Fermi surface" of Ag–25 at. % Mg in (a) the ΓXKX and (b) $\Gamma XULK$ planes. In (a) the solid line is for the empty lattice approximation.

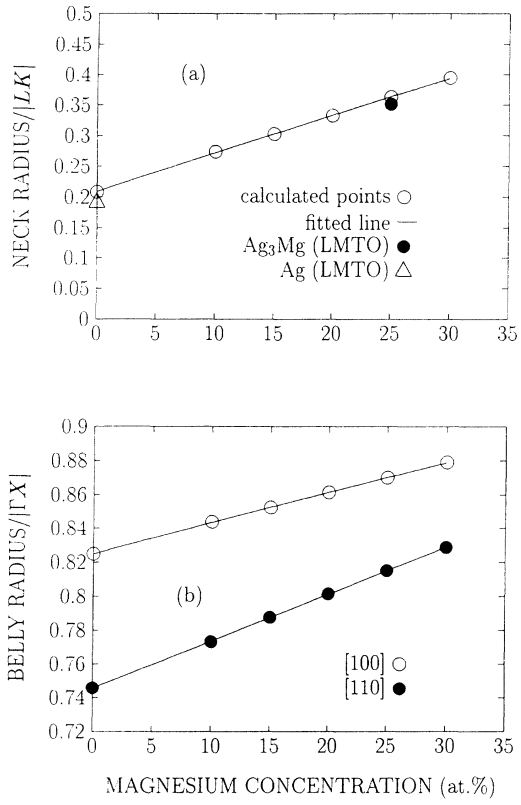

FIG. 9. The variation of (a) the neck radius at the L point and (b) the belly radii along ΓX and ΓK, with Mg concentration.

alloys has an important influence on various properties. Since we have already examined some aspects and consequences of certain features in earlier papers, such as the flattening that occurs between the L points,[6–8] we will not discuss them in any detail here. However, we should point out briefly that we believe that "nesting" can occur between the flattened, parallel regions in the ⟨110⟩ directions, giving rise to concentration waves for which the electronic structure of the homogeneous state, described by the KKR-CPA, is unstable and whose wave vectors are determined by the nesting vectors. As a result a fourfold set of intensity maxima (satellites) occur in the diffuse scattering from the alloys around the (100), (110) and equivalent, positions. The magnitude of the nesting vector is twice the belly radius in the ΓK direction and so we can see from Fig. 9(b) that it depends sensitively on the Mg content. Thus, the wave vector of the concentration wave, and the separation of the satellite peaks in the diffuse scattering, are composition dependent. In fact, the variation of the peak separation we calculated[6,8] is in excellent agreement with the observations of Ohshima and Watanabe.[5] Furthermore, the intensity maxima in the diffuse scattering are precursors to the formation of the ordered LPS structures since they become sharper and eventually develop into Bragg peaks as the long range order sets in. In the case of Ag-Mg alloys the LPS periods are incommensurate and we have obtained excellent agreement between the observed average domain size, i.e., the average number of $L1_2$ units per domain, and that given by the calculations.[7]

IV. SUMMARY

In this paper, we report calculations of the electronic structure of the valence bands in a series of α-phase (disordered fcc) Ag-Mg alloys in the range 0–30 at.% Mg using the LDA-KKR-CPA. We find that the variation of the equilibrium lattice constants is in good agreement with that observed experimentally. The valence bands are dominated by the Ag 4*d*-related states and we find that the bandwidth decreases with increasing Mg concentration although the bottom of the bands remains fixed in energy, with reference to the Fermi level; a result that is consistent with *uv* photoemission measurements of a 25 at.% Mg alloy. The calculations of the electronic spectral densities indicate that states with *s* and *p* character are much less disorder broadened than *d* states and that at the Fermi energy the peaks in the spectral functions are sharp, with widths that are considerably less than 1% of the Brillouin zone dimension. Thus, the Fermi surfaces are well defined. We show that the radius of the neck at the L point and the belly radii increase very nearly linearly with Mg concentration. In previous papers in which we examined the changes in the dimensions of the Fermi surface, we concluded that the agreement between our calculations and the experimental results not only provided strong evidence that Fermi surface features play an important role in establishing the short range and long range order in α-phase Ag-Mg alloys, but also the results demonstrated the accuracy of the KKR-CPA in dealing with the phenomenon of incommensurate concentration waves. The additional areas of agreement between the calculations described here and the experimentally measured lattice constants and photoemission measurements give further support to the conclusion that the LDA-KKR-CPA provides a realistic description of the electronic structures in Ag-rich Ag-Mg alloys.

ACKNOWLEDGMENTS

This work was supported by funds from the National Science Foundation, Contract No. DMR-9120120 (to R.G.J. and S.L.Q.), from the Southeastern Universities Research Association (R.G.J.) as part of the SURA/ORNL materials program, by the Division of Materials Sciences (G.M.S.), Office of Basic Energy Science, and the Applied Mathematical Sciences Program (W.A.S.), Office of Energy Research, USDOE, under Subcontract No. DE-AC05-84OR21400 with Martin Marietta Energy Systems, Inc. R.G.J. and Y.L. thank members of the Metals and Ceramics Division at ORNL for their kind hospitality. R.G.J. and S.L.Q. are grateful to Florida State University for the provision of CRAY supercomputer resources and Y.L. wishes to express her thanks to the Department of Physics, Florida Atlantic University for partial financial support.

* Present address: Physics Department, Brookhaven National Laboratory, Upton, New York 11973-5000

[1] *Binary Alloy Phase Diagrams*, edited by T.B. Massalski (American Society for Metals, Ohio, 1986).
[2] K. Schubert, B. Kiefer, M. Wilkens, and R. Haufler, Z. Metallk. **46**, 692 (1955). See also Ref. 10.
[3] See, for example, K. Girgis, in *Physical Metallurgy, Part 1*, edited by R.W. Cahn and P. Haasen (North-Holland, Amsterdam, 1983), p. 220; T.B. Massalski, *ibid.*, p. 153.
[4] Yan Liu, R.G. Jordan, and S.L. Qiu, Phys. Rev. B **49**, 4478 (1994).
[5] K. Ohshima and D. Watanabe, Acta Crystallogr. Sec. A **33**, 784 (1977).
[6] Yan Liu, R.G. Jordan, S.L. Qiu, and G.M. Stocks, in *Metallic Alloys: Experimental and Theoretical Perspectives,* Vol. 256 of *NATO Advanced Study Institute, Series E: Applied Sciences*, edited by J.S. Faulkner and R.G. Jordan, (Kluwer Academic, Dordrecht, 1994), p. 225.
[7] R.G. Jordan, in *Alloy Modeling and Design*, edited by G.M. Stocks and P.E.A. Turchi (TMS, Pittsburgh, in press).
[8] R.G. Jordan, Yan Liu, S.L. Qiu, G.M. Stocks, W.A. Shelton, and B. Ginatempo, Acta Metall. Mater. (to be published).
[9] J.S. Faulkner and G.M. Stocks, Phys. Rev. B **21**, 3222 (1980).
[10] K. Fujiwara, M. Hirabayashi, D. Watanabe, and S. Ogawa, J. Phys. Soc. Jpn. **13**, 167 (1958).
[11] R.A. Buckley, H.J. Axon, and J. Conacher, J. Inst. Met. **88**, 225 (1959).
[12] Yan Liu, Ph.D. thesis, Florida Atlantic University, 1993.
[13] L.T. Wille and P.J. Durham, Surf. Sci. **164**, 19 (1985).
[14] R.G. Jordan, Vacuum **33**, 827 (1983). See also R.G. Jordan and P.J. Durham, Solid State Commun. **49**, 623 (1984).
[15] R.G. Jordan and G.S. Sohal, J. Phys. C **15**, L663 (1982).